Journal of Solid State Chemistry **167,** 41–47 (2002)
doi:10.1006/jssc.2002.9616

Lanthanum Gallium Tin Antimonides $LaGa_xSn_ySb_2$

Mark G. Morgan, Meitian Wang, Allison M. Mills, and Arthur Mar[1]

Department of Chemistry, University of Alberta, Edmonton, Alberta, Canada T6G 2G2

Received February 1, 2000; in revised form March 28, 2002; accepted April 12, 2002

A series of quaternary lanthanum gallium tin antimonides $LaGa_xSn_ySb_2$ was elaborated to trace the structural evolution between the known end members $LaGaSb_2$ ($SmGaSb_2$-type) and $LaSn_ySb_2$ ($LaSn_{0.75}Sb_2$-type). Five members of this series were characterized by single-crystal X-ray diffraction. For low Sn content, the Sn atoms disorder with Ga atoms in zigzag chains to form solid solutions $LaGa_{1-y}Sn_ySb_2$ ($0 \le y \le 0.2$) adopting the $SmGaSb_2$-type structure, as exemplified by $LaGa_{0.92(3)}Sn_{0.08}Sb_2$ and $LaGa_{0.80(3)}Sn_{0.20}Sb_2$ (orthorhombic, space group $D_2^5 - C222_1$, $Z = 4$). For higher Sn and lower Ga content, there is a segregation in which the Sn atoms appear in chains of closely spaced partially occupied sites as in the parent $LaSn_{0.75}Sb_2$-type structure whereas the Ga atoms remain in zigzag chains as in the parent $SmGaSb_2$-type structure. This feature is observed in the structures of $LaGa_{0.68(4)}Sn_{0.31(3)}Sb_2$, $LaGa_{0.62(3)}Sn_{0.32(3)}Sb_2$, and $LaGa_{0.43(3)}Sn_{0.39(3)}Sb_2$ (orthorhombic, space group $D_{2h}^{17} - Cmcm$, $Z = 4$). The last example illustrates that the combined Ga/Sn content can be substoichiometric ($x + y < 1$). These compounds have a layered nature, with the chains of Ga or Sn atoms residing between $^2_\infty[LaSb_2]$ slabs. © 2002 Elsevier Science (USA)

Key Words: **antimonide; gallium; tin; structure.**

INTRODUCTION

The structures of ternary rare-earth antimonides with the composition $REMSb_2$ can be considered as being built up by stacking $^2_\infty[RESb_2]$ slabs, followed by insertion of M atoms between these slabs (1–10). Although this partitioning may seem somewhat artificial, it provides a connection to the structures of known rare-earth diantimonides $RESb_2$ (11–13). The M atoms tend to be late d-block or post-transition-metal elements, and they form networks involving M–M bonding in square sheets (e.g., $LaCd_{0.7}Sb_2$ (7)) or zigzag chains (e.g., $LaIn_{0.8}Sb_2$ (9), $REGaSb_2$ (10)). There is frequently a significant substoichiometry in M, implying that the M–M bonding networks are randomly severed into finite segments. Although phase transitions in solid-state compounds, when they occur, are typically induced by temperature or pressure changes, it is also of interest to study how progressive compositional changes may cause these M–M bonding networks to distort.

The similarity of the structures of $LaGaSb_2$ ($C222_1$) (10) and $LaSn_{0.75}Sb_2$ ($Cmcm$) (8) prompted us to investigate the quaternary system $LaGa_xSn_ySb_2$. The $^2_\infty[LaSb_2]$ slabs are stacked in an identical sequence in $LaGaSb_2$ and $LaSn_{0.75}Sb_2$. Running along the c-direction are zigzag chains of Ga atoms in $LaGaSb_2$ or slightly undulating linear chains of partially occupied Sn sites in $LaSn_{0.75}Sb_2$. A substantial range of nonstoichiometry occurs in $LaSn_ySb_2$, with $\sim 0.1 \le y \le \sim 0.7$. We were interested in determining whether the transition from zigzag chains to linear chains takes place through gradual distortion of the M–M bonding network, or whether it occurs abruptly at some critical Ga/Sn ratio. Here we report the structures of five representative members in the $LaGa_xSn_ySb_2$ series, and demonstrate that the structural transition of the M–M bonding network proceeds through an alternative means.

EXPERIMENTAL

Synthesis

Starting materials were La powder (99.9%, Alfa-Aesar), crushed Ga granules (99.9999%, Alfa-Aesar), Sn powder (99.8%, Cerac), and Sb powder (99.995%, Aldrich). Reactions were performed on a 0.25-g scale in evacuated fused-silica tubes (8-cm length; 10-mm i.d.). Generally, successful syntheses involved heating at temperatures between 850°C and 950°C for 2–3 days, cooling to 500°C over 1–4 days, and cooling to 20°C over several hours. Products were analyzed by powder X-ray diffraction on an Enraf-Nonius FR552 Guinier camera, and elemental compositions of crystals were determined by energy-dispersive X-ray (EDX) analysis on a Hitachi S-2700 scanning electron microscope.

Quaternary $LaGa_xSn_ySb_2$ compounds were originally identified as side products in attempts to grow single crystals of $La_{13}Ga_8Sb_{21}$ (14) and $LaGaSb_2$ (10) through the use of a Sn flux. Because the morphologies and

[1]To whom correspondence should be addressed. Fax: 780-492-8231. E-mail: arthur.mar@ualberta.ca.

0022-4596/02 $35.00

compositions of these crystals are so similar, careful screening by Weissenberg photography and EDX analysis was essential. Stoichiometric reaction of the elements was only successful for the most Ga-rich members. For example, the reaction of La, Ga, Sn, and Sb in the ratio 1.0:0.8:0.2:2.0 produced single crystals of $LaGa_{0.8}Sn_{0.2}Sb_2$. However, reaction of the same elements in the ratio 1.0:0.6:0.4:2.0 did not produce $LaGa_{0.6}Sn_{0.4}Sb_2$, but rather a solid solution $La_{12}Ga_{4-x}Sn_xSb_{23}$ adopting the $Pr_{12}Ga_4Sb_{23}$-type structure in which Ga and Sn atoms are disordered (14). Moreover, the crystals tended to be small in these stoichiometric reactions. Use of either excess Ga or excess Sn aided crystal growth, but only in the latter case were quaternary $LaGa_xSn_ySb_2$ crystals preferentially formed. Considerable variation in the compositions of these crystals led us to select a few representative members, prescreened by EDX analyses, for structure determination. The ultimate compositions of selected crystals were determined from the structure refinements and were consistent with individual EDX analyses. For example, the crystal refined as $LaGa_{0.8}Sn_{0.2}Sb_2$ has a composition in good agreement with its EDX analysis (Anal. (mol %) Calcd: 25% La, 20% Ga, 5% Sn, 50% Sb. Found: 25(1)% La, 18(1)% Ga, 7(1)% Sn, 51(2)% Sb). Generally, the refined compositions were within 1–2% of the EDX analyses, which can have uncertainties up to 4–5%.

Structure Determination

Preliminary cell parameters were obtained by Weissenberg photography. Intensity data were collected at 22°C with Mo$K\alpha$ radiation (0.71073 Å) by ω scans (0.2°) on a Bruker Platform/SMART 1000 CCD diffractometer. Crystal data and further details of the data collection are given in Table 1. All calculations were performed with use of the SHELXTL (Version 5.1) package (15). Conventional atomic scattering factors and anomalous dispersion corrections were used (16). Intensity data were reduced and averaged with SAINT 6.0, and face-indexed numerical absorption corrections were applied with XPREP.

The space groups $C222_1$ (adopted by $SmGaSb_2$ type (10)) and *Cmcm* (adopted by $LaSn_{0.75}Sb_2$ type (8)) are distinguishable by the occurrence of the systematic absences $h0l, l = 2n + 1$ in the latter. For example, in $LaGa_{0.9}Sn_{0.1}Sb_2$, the 32 reflections of the form $h0l, l = 2n + 1$ had $\langle I/\sigma \rangle = 8.6$ (compared to $\langle I/\sigma \rangle = 17.8$ for all reflections) and 23 of these had $I > 3\sigma(I)$. In contrast, in $LaGa_{0.6}Sn_{0.3}Sb_2$, the 11 reflections of this form had $\langle I/\sigma \rangle = 3.7$ (compared to $\langle I/\sigma \rangle = 12.8$ for all reflec-

TABLE 1
Crystallographic Data for $LaGa_xSn_ySb_2$

Formula	$LaGa_{0.92(3)}Sn_{0.08}Sb_2$	$LaGa_{0.80(3)}Sn_{0.20}Sb_2$	$LaGa_{0.68(4)}Sn_{0.31(3)}Sb_2$	$LaGa_{0.62(3)}Sn_{0.32(3)}Sb_2$	$LaGa_{0.43(3)}Sn_{0.39(3)}Sb_2$
Formula mass (amu)	456.41	461.92	466.82	463.62	457.77
Space group	$D_2^5-C222_1$ (No.20)	$D_2^5-C222_1$ (No.20)	$D_{2h}^{17}-Cmcm$ (No.63)	$D_{2h}^{17}-Cmcm$ (No.63)	$D_{2h}^{17}-Cmcm$ (No.63)
a (Å)[a]	4.3920(4)	4.3817(8)	4.3783(2)	4.3752(2)	4.3728(5)
b (Å)[a]	22.930(2)	22.909(4)	23.0173(9)	23.0095(10)	23.029(3)
c (Å)[a]	4.4138(4)	4.4032(8)	4.4224(2)	4.4184(2)	4.4197(5)
V (Å^3)	444.51(7)	441.99(14)	445.67(3)	441.81(3)	445.06(9)
Z	4	4	4	4	4
ρ_{calcd} (g cm^{-3})	6.820	6.942	6.957	6.923	6.832
Crystal dimensions (mm)	$0.180 \times 0.028 \times 0.012$	$0.296 \times 0.036 \times 0.028$	$0.432 \times 0.130 \times 0.012$	$0.188 \times 0.050 \times 0.018$	$0.264 \times 0.064 \times 0.038$
μ(Mo$K\alpha$) (cm^{-1})	271.73	272.79	270.09	266.97	258.16
Transmission factors	0.253–0.724	0.094–0.479	0.035–0.723	0.126–0.585	0.064–0.370
2θ Limits	7.10–66.20	3.56–65.22	3.54–65.12	3.54–65.30	3.54–65.16
Data collected	$-6 \le h \le 6, -33 \le k \le 34, -6 \le l \le 5$	$-6 \le h \le 6, -34 \le k \le 31, -6 \le l \le 3$	$-6 \le h \le 6, -34 \le k \le 34, -6 \le l \le 6$	$-6 \le h \le 6, -34 \le k \le 32, -6 \le l \le 6$	$-5 \le h \le 6, -23 \le k \le 34, -6 \le l \le 6$
No. of data collected	2551	2068	2550	2590	1762
No. of unique data, including $F_o^2 < 0$	815	804	492	497	494
No. of unique data, with $F_o^2 > 2\sigma(F_o^2)$	780	758	489	477	483
No. of variables	25	24	26	26	26
$R(F)$ for $F_o^2 > 2\sigma(F_o^2)$[b]	0.030	0.073	0.056	0.051	0.052
$R_w(F_o^2)$[c]	0.076	0.182	0.141	0.130	0.141
Goodness of fit	1.126	1.101	1.241	1.169	1.219
$(\Delta\rho)_{max}$, $(\Delta\rho)_{min}$ (e Å^{-3})	3.41, −1.97	7.85, −6.57	4.37, −3.87	4.61, −4.55	6.04, −4.30

[a] Obtained from a refinement constrained so that $\alpha = \beta = \gamma = 90°$.
[b] $R(F) = \sum||F_o| - |F_c||/\sum|F_o|$.
[c] $R_w(F_o^2) = [\sum w(F_o^2 - F_c^2)^2/\sum wF_o^4]^{1/2}$; $w^{-1} = [\sigma^2(F_o^2)+(ap)^2+bp]$, where $p = [\max(F_o^2, o)+2F_c^2]/3$.

tions) and only three of these had $I > 3\sigma(I)$. The violations of the *c*-glide absences favor the choice of space group $C222_1$ for $LaGa_{0.9}Sn_{0.1}Sb_2$ and $LaGa_{0.8}Sn_{0.2}Sb_2$, whereas space group *Cmcm* was chosen for the remaining three crystals. The initial positions of the La and Sb atoms in all structures were taken from those in $SmGaSb_2$ or $LaSn_{0.75}Sb_2$. Appreciable electron density remaining between the $^2_\infty[LaSb_2]$ slabs was assigned as Ga or Sn atoms. In the two Ga-rich members, only one site, which forms zigzag chains aligned along the *c*-direction, is found between the slabs. This site was allowed to be occupied by a mixture of Ga and Sn atoms, with the constraint that the occupancies sum up to 100%. The refinements converged to give reasonable values for the occupancies so that the final crystallographic formulas $LaGa_{0.92(3)}Sn_{0.08}Sb_2$ and $LaGa_{0.80(3)}Sn_{0.20}Sb_2$ are consistent with the compositions determined by EDX analyses. In the remaining crystals, several sites between the $^2_\infty[LaSb_2]$ slabs are found. One site generates two sets of zigzag chains related by a mirror plane so that the maximum occupancy is 50% (similar to the situation in $NdGaSb_2$ (10)). Three other sites (all having $x = 0$) generate a linear chain parallel to the zigzag chains. By analogy with the parent end-member structures, the sites in the zigzag chains were occupied by Ga atoms and those in the linear chains by Sn atoms. When the occupancies of these sites were refined, with no constraints placed on the sum of the occupancies, they converged to reasonable values, giving formulas $LaGa_{0.68(4)}Sn_{0.31(3)}Sb_2$, $LaGa_{0.62(3)}Sn_{0.32(3)}Sb_2$, and $LaGa_{0.43(3)}Sn_{0.39(3)}Sb_2$ that are consistent with the EDX analyses. In all five structures, the sites containing Ga and Sn atoms were refined with isotropic displacement parameters only.

The structures of $LaGa_{0.92(3)}Sn_{0.08}Sb_2$ and $LaGa_{0.80(3)}Sn_{0.20}Sb_2$ exhibit a pseudosymmetry such that they can also be refined in space group *Cmcm*, notwithstanding the observed violations of the *c*-glide absences. This treatment entails a disorder in sites, each with a maximum 50% occupancy, within two zigzag chains related by a mirror plane. We opt to retain the solution in $C222_1$, in which the disorder of the zigzag chains is accounted for by the occurrence of racemic twinning in a 0.4(1)/0.6 fraction in both crystals.

The largest residuals in the difference electron density maps are 7.85 and $-6.57\,e\,Å^{-3}$ located 0.70 and 1.18 Å away, respectively, from the La atom in $LaGa_{0.92(3)}Sn_{0.08}Sb_2$, and 6.04 and $-4.30\,e\,Å^{-3}$ located 1.30 Å away from the Ga atom and 0.39 Å away from the Sn(1) atom, respectively, in $LaGa_{0.43(3)}Sn_{0.39(3)}Sb_2$. In the other structures, the difference electron density maps are featureless, with less pronounced residuals. The atomic positions in the five structures were standardized with the program STRUCTURE TIDY (17). Final values of the positional and displacement parameters are given in Table 2. Interatomic distances are listed in Table 3. Further data, in the form of a CIF, have been sent to Fachinformationszentrum Karlsruhe, Abt. PROKA, 76344 Eggenstein-Leopoldshafen, Germany, as supplementary material No. CSD– 412480–412484 and can be obtained by contacting FIZ (quoting the article details and the corresponding CSD numbers).

RESULTS AND DISCUSSION

For simplicity, we refer to the five quaternary compounds by the formulas $LaGa_{0.9}Sn_{0.1}Sb_2$, $LaGa_{0.8}Sn_{0.2}Sb_2$, $LaGa_{0.7}Sn_{0.3}Sb_2$, $LaGa_{0.6}Sn_{0.3}Sb_2$, and $LaGa_{0.4}Sn_{0.4}Sb_2$. Their structures are related, consisting of $^2_\infty[LaSb_2]$ slabs separated by chains of Ga and Sn atoms (Figs. 1 and 2). The $^2_\infty[LaSb_2]$ slabs, each approximately 10 Å thick, are stacked along the long *b*-axis. These slabs are made up of a central square net of Sb(2) atoms and two square nets, half as dense, of Sb(1) atoms; La atoms reside in square antiprismatic sites above and below the Sb(2) square net. The five compounds can be separated into two structure types: (a) $SmGaSb_2$ type ($LaGa_{0.9}Sn_{0.1}Sb_2$, $LaGa_{0.8}Sn_{0.2}Sb_2$) and (b) a disordered structure that has features of both the $SmGaSb_2$ and $LaSn_{0.75}Sb_2$ types ($LaGa_{0.7}Sn_{0.3}Sb_2$, $LaGa_{0.6}Sn_{0.3}Sb_2$, $LaGa_{0.4}Sn_{0.4}Sb_2$).

When only a small amount of Sn is added in $LaGa_{1-y}Sn_ySb_2$, the parent $LaGaSb_2$ ($SmGaSb_2$ type) structure (10) is retained (Fig. 1). In $LaGaSb_2$, the Ga atoms form zigzag chains running along the *c* direction. Each Ga atom is coordinated by two other Ga atoms and two Sb(1) atoms in a distorted tetrahedral fashion. In $LaGa_{0.9}Sn_{0.1}Sb_2$ and $LaGa_{0.8}Sn_{0.2}Sb_2$, the zigzag chains consist of a disordered mixture of Ga and Sn atoms. With the low amount of Sn present, most of the contacts within the zigzag chains are Ga–Ga bonds, with a small proportion of Ga–Sn bonds. The interatomic distances within these zigzag chains are 2.591(3)–2.594(2) Å, somewhat longer than typical Ga–Ga bonds found in $SmGaSb_2$ (2.539(2) Å) (10) and $Na_2Ga_3Sb_3$ (2.541(3) Å) (18) and somewhat shorter than typical Ga–Sn bonds found in $NaGaSn_5$ (2.764(4)–2.783(2) Å) (19) although Ga–Sn bonds as short as 2.448 Å are implied in a Sn-doped GaAs (20). The (Ga/Sn)–Sb(1) distances are 2.782(2)–2.789(1) Å, similar to the Ga–Sb bonds found in $SmGaSb_2$ (2.761(1) Å) (10) and slightly shorter than the Sn–Sb bonds found in Na_5SnSb_3 (2.805(1)–2.945(1) Å) (21). If larger amounts of Sn are introduced into the zigzag chains, unreasonably short Sn–Sn contacts would result. Although the bond lengths are still reasonable when a small amount of Sn atoms occupies the sites in the zigzag chains, the competing effects of less than optimum Ga–Ga, Ga–Sn, Ga–Sb, and Sn–Sb bonding give rise to only a narrow range of solid solution in $LaGa_{1-y}Sn_ySb_2$ ($0 \le y \le \sim 0.2$).

TABLE 2
Positional and Equivalent Isotropic Displacement Parameters for $LaGa_xSn_ySb_2$

Atom	Wyckoff position	x	y	z	Occupancy	U_{eq} or U_{iso} (Å^2)[a]
$LaGa_{0.92(3)}Sn_{0.08}Sb_2$						
La	4*b*	0	0.13889(2)	$\frac{1}{4}$	1	0.0080(2)
Sb(1)	4*b*	0	0.40991(3)	$\frac{1}{4}$	1	0.0099(2)
Sb(2)	4*b*	0	0.75013(2)	$\frac{1}{4}$	1	0.0092(2)
Ga/Sn	4*a*	0.1551(4)	0	0	0.92(3)/0.08	0.0276(6)
$LaGa_{0.80(3)}Sn_{0.20}Sb_2$						
La	4*b*	0	0.13889(3)	$\frac{1}{4}$	1	0.0080(3)
Sb(1)	4*b*	0	0.40993(4)	$\frac{1}{4}$	1	0.0099(3)
Sb(2)	4*b*	0	0.75018(4)	$\frac{1}{4}$	1	0.0094(3)
Ga/Sn	4*a*	0.1559(6)	0	0	0.80(3)/0.20	0.0293(7)
$LaGa_{0.68(4)}Sn_{0.31(3)}Sb_2$						
La	4*c*	0	0.13940(5)	$\frac{1}{4}$	1	0.0095(4)
Sb(1)	4*c*	0	0.40952(7)	$\frac{1}{4}$	1	0.0121(4)
Sb(2)	4*c*	0	0.75021(6)	$\frac{1}{4}$	1	0.0106(4)
Ga	8*e*	0.157(3)	0	0	0.34(2)	0.040(3)
Sn(1)	8*f*	0	−0.0047(9)	0.130(8)	0.10(2)	0.034(8)
Sn(2)	4*c*	0	−0.0070(17)	$\frac{1}{4}$	0.06(3)	0.023(16)
Sn(3)	4*a*	0	0	0	0.04(2)	0.010(19)
$LaGa_{0.62(3)}Sn_{0.32(3)}Sb_2$						
La	4*c*	0	0.13945(5)	$\frac{1}{4}$	1	0.0088(3)
Sb(1)	4*c*	0	0.40945(6)	$\frac{1}{4}$	1	0.0114(3)
Sb(2)	4*c*	0	0.75024(5)	$\frac{1}{4}$	1	0.0097(3)
Ga	8*e*	0.154(3)	0	0	0.31(2)	0.044(4)
Sn(1)	8*f*	0	−0.0050(7)	0.128(6)	0.11(1)	0.029(6)
Sn(2)	4*c*	0	−0.0070(12)	$\frac{1}{4}$	0.06(2)	0.017(11)
Sn(3)	4*a*	0	0	0	0.05(2)	0.014(16)
$LaGa_{0.43(3)}Sn_{0.39(3)}Sb_2$						
La	4*c*	0	0.13952(4)	$\frac{1}{4}$	1	0.0088(4)
Sb(1)	4*c*	0	0.40935(5)	$\frac{1}{4}$	1	0.0113(4)
Sb(2)	4*c*	0	0.75023(5)	$\frac{1}{4}$	1	0.0096(4)
Ga	8*e*	0.151(4)	0	0	0.21(2)	0.042(5)
Sn(1)	8*f*	0	−0.0050(5)	0.126(4)	0.13(1)	0.028(4)
Sn(2)	4*c*	0	−0.0071(8)	$\frac{1}{4}$	0.08(2)	0.017(8)
Sn(3)	4*a*	0	0	0	0.05(2)	0.016(13)

[a] U_{eq} is defined as one-third of the trace of the orthogonalized U_{ij} tensor. Sites containing Ga and Sn atoms were refined with isotropic displacement parameters only.

When a larger amount of Sn and a smaller amount of Ga are present, a hybrid structure results (Fig. 2). The Ga atoms remain in zigzag chains, but the change to space group *Cmcm* introduces a disorder of these chains into two possible configurations so that the maximum occupancy is 50%, similar to the situation in the $NdGaSb_2$-type structure (10). On going from $LaGa_{0.7}Sn_{0.3}Sb_2$ to $LaGa_{0.4}Sn_{0.4}Sb_2$, the reduction in Ga content occurs by gradual introduction of vacancies into the Ga zigzag chains. The Sn atoms can no longer be accommodated in the zigzag chains, but they reappear in slightly undulating linear chains containing three kinds of closely spaced partially occupied sites, as in the parent $LaSn_{0.75}Sb_2$-type structure. As discussed elsewhere (8), the Sn atoms must be spaced at least $\sim$2.8 Å apart (corresponding to a reasonable Sn–Sn bond), i.e., a local distribution of Sn atoms occupying every fifth site or further, giving randomly segmented Sn–Sn chains. The observed occupancies range from 4(2)% to 13(1)% in these Sn sites. Each Sn atom is also coordinated to two or four surrounding Sb atoms at reasonable Sn–Sb contacts (2.91(1)–3.219(1) Å). Both types of chains are aligned along the *c*-direction, but there is disorder between Ga and Sn chains. Since related layered structures are prone to stacking disorder, a reasonable interpretation is that there is a random distribution of domains of Ga and Sn chains, resulting in an average structure. Local inhomogeneities during the synthesis would also

TABLE 3
Selected Interatomic Distances (Å) in $LaGa_xSn_ySb_2$

	$LaGa_{0.92(3)}Sn_{0.08}Sb_2$	$LaGa_{0.80(3)}Sn_{0.20}Sb_2$	$LaGa_{0.68(4)}Sn_{0.31(3)}Sb_2$	$LaGa_{0.62(3)}Sn_{0.32(3)}Sb_2$	$LaGa_{0.43(3)}Sn_{0.39(3)}Sb_2$
La–Sb(1) (× 4)	3.3084(3)	3.3012(6)	3.3091(7)	3.3064(6)	3.3061(6)
La–Sb(2) (× 2)	3.3658(6)	3.3615(10)	3.3612(14)	3.3592(13)	3.3587(11)
La–Sb(2) (× 2)	3.3684(6)	3.3622(10)	3.3682(14)	3.3649(12)	3.3659(11)
La–Ga (× 2)	3.4388(6)[a]	3.4355(11)[a]	3.463(3)	3.460(3)	3.461(4)
La–Sn(1) (× 2)	—	—	3.36(2)	3.37(1)	3.37(1)
La–Sn(1) (× 2)	—	—	3.53(2)	3.52(2)	3.51(1)
La–Sn(2)	—	—	3.37(4)	3.37(3)	3.38(2)
La–Sn(2) (× 2)	—	—	3.76(3)	3.76(2)	3.76(1)
La–Sn(3) (× 2)	—	—	3.394(1)	3.394(1)	3.398(1)
Ga–Ga (× 2)	2.594(2)[a]	2.591(3)[a]	2.603(13)	2.587(15)	2.573(18)
Ga–Sb(1) (× 2)	2.789(1)[a]	2.782(2)[a]	2.796(7)	2.803(8)	2.813(10)
Sb(2)–Sb(2) (× 4)	3.1133(2)	3.1060(4)	3.1116(1)	3.1091(1)	3.1087(3)
Sn(1)–Sb(1) (× 2)	—	—	3.00(1)	2.99(1)	2.994(8)
Sn(2)–Sb(1) (× 2)	—	—	2.91(3)	2.91(2)	2.91(1)
Sn(3)–Sb(2) (× 4)	—	—	3.2174(10)	3.2166(9)	3.2186(8)
Sn(1)–Sn(2)	—	—	2.75(4)	2.76(3)	2.77(2)
Sn(1)–Sn(3)	—	—	2.79(4)	2.78(3)	2.77(2)

[a] In $LaGa_{0.92(3)}Sn_{0.08}Sb_2$ and $LaGa_{0.80(3)}Sn_{0.20}Sb_2$, these values refer to distances to the disordered sites containing 0.92(3) Ga/0.08 Sn and 0.80(3) Ga/0.20 Sn, respectively.

give rise to variations in the compositions of these crystals. Because the Ga chains and Sn chains are assumed to be independent of each other, the sum of their occupancies need not be equal to one. For example, $LaGa_{0.4}Sn_{0.4}Sb_2$ shows considerable substoichiometry in both the Ga and Sn chains.

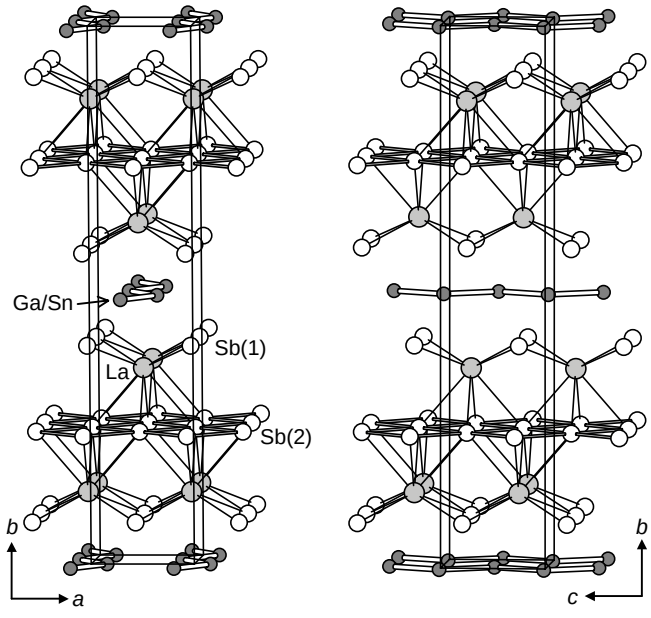

FIG. 1. Views (a) down the *c*-axis and (b) down the *a*-axis of the structure of $LaGa_{0.9}Sn_{0.1}Sb_2$ or $LaGa_{0.8}Sn_{0.2}Sb_2$ ($SmGaSb_2$ type), showing the unit-cell outline and the labeling scheme. The large lightly shaded circles are La atoms, the small solid circles are sites containing a disordered mixture of Ga and Sn atoms, and the medium open circles are Sb atoms.

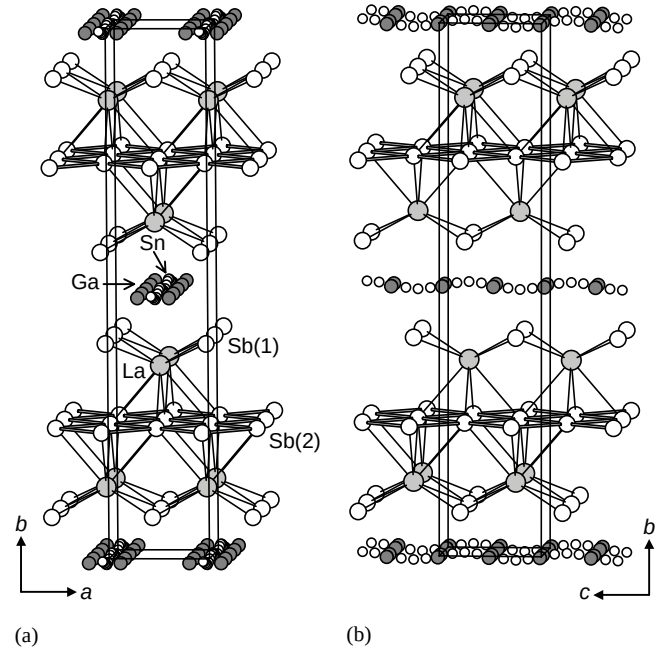

FIG. 2. Views (a) down the *c*-axis and (b) down the *a*-axis of the structure of $LaGa_{0.7}Sn_{0.3}Sb_2$, $LaGa_{0.6}Sn_{0.3}Sb_2$, or $LaGa_{0.4}Sn_{0.4}Sb_2$, showing the unit-cell outline and the labeling scheme. The large lightly shaded circles are La atoms, the small solid circles are partially occupied sites containing Ga atoms (21–34% occupancy), the small open circles are partially occupied sites containing Sn atoms (4–13% occupancy), and the medium open circles are Sb atoms.

The quaternaries $LaGa_xSn_ySb_2$ thus represent a continuum of structures, as shown in Fig. 3. $LaGa_{1-y}Sn_ySb_2$ ($0 \le y \le \sim 0.2$) contains only zigzag chains that are occupied fully by a mixture of Ga and a small amount of Sn atoms (Fig. 3a); intermediate members $LaGa_xSn_ySb_2$ contain separate, partially occupied zigzag chains of Ga atoms and linear chains of Sn atoms (Fig. 3b); $LaSn_ySb_2$ contains only partially occupied chains of Sn atoms (Fig. 3c). Given the significant degree of disorder and nonstoichiometry, it is difficult to provide a simple bonding scheme for these quaternary antimonides. Application of the Zintl concept suggests an initial formulation $La^{3+}[Ga_xSn_ySb(1)]^{2-}[Sb(2)]^{1-}$, where the Sb(2) atoms in a square net form four $\sim$3.11 Å Sb–Sb bonds of approximately one-half bond order ("one-electron bonds"), consistent with the nonclassical bonding found in many antimonide substructures (22–24). Although electronic structures for disordered systems such as these are problematic to determine, we can extrapolate from the band structure of the composite $[GaSb_2]^{3-}$ substructure in the parent $RE GaSb_2$, which has been calculated previously (10). It was noted that additional Ga–Ga bonding levels could still be occupied without severely weakening the Sb–Sb bonding within the Sb(2) square net, leading to the prediction that Ga could be substituted with a more electron-rich element. The elaboration of the solid solution $LaGa_{1-y}Sn_ySb_2$ demonstrates that this is indeed possible, although the degree of substitution is limited ($0 \le y \le \sim 0.2$). A rigid band model becomes unrealistic if large amounts of Sn are added. The higher (less negative) energies of the $s-p$ orbitals of Sn compared to Ga raises the Sn–Sn bonding levels relative to the Ga–Ga bonding levels. The Sb–Sb levels, however, remain unchanged. To preclude occupation of Sb–Sb antibonding levels that would ensue if too many electrons were added through substitution of Sn for Ga, the Sn content remains substoichiometric. The segregation into separate Ga chains and Sn chains probably occurs on steric grounds, since maintaining Ga–Ga, Ga–Sn, and Sn–Sn bonds of equal lengths within a single type of chain would become impossible. A steric effect is also manifested by an increasing distortion of the square net of Sb(2) atoms to which the Ga and Sn atoms are bonded; the Sb(2)–Sb(2)–Sb(2) angles progress from 89.7–90.3° in the Ga-rich members ($LaGa_{0.9}Sn_{0.1}Sb_2$ and $LaGa_{0.8}Sn_{0.2}Sb_2$), to 89.4–90.6° in the more Sn-rich members ($LaGa_{0.7}Sn_{0.3}Sb_2$, $LaGa_{0.6}Sn_{0.3}Sb_2$, and $LaGa_{0.4}Sn_{0.4}Sb_2$), and finally to 86.6–93.4° in the all-Sn extreme ($LaSn_{0.75}Sb_2$) (8). However, we cannot rule out the possibility that a small amount of Sn can mix into the Ga chains, or a small amount of Ga can mix into the Sn chains.

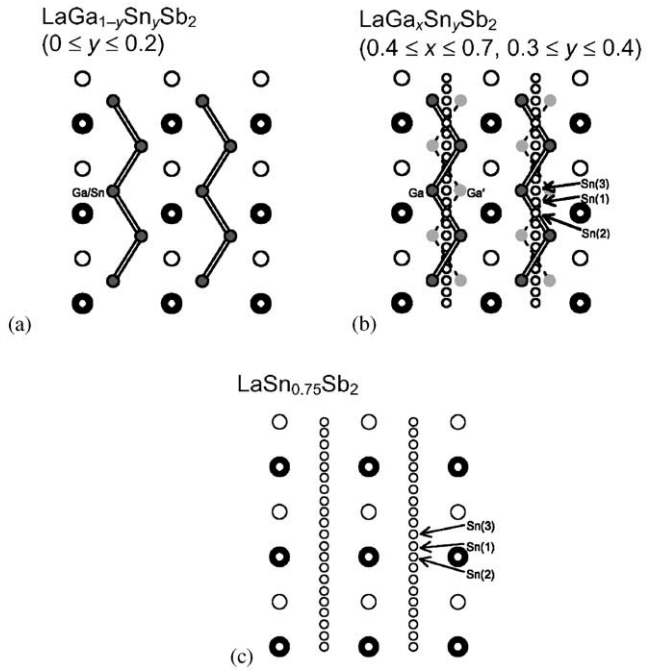

FIG. 3. Evolution of Ga and Sn chains, inserted between two square nets of Sb atoms (shown with thick and thin rims, respectively) viewed down the *b*-axis, in (a) $LaGa_{0.9}Sn_{0.1}Sb_2$ and $LaGa_{0.8}Sn_{0.2}Sb_2$; (b) $LaGa_{0.7}Sn_{0.3}Sb_2$, $LaGa_{0.6}Sn_{0.3}Sb_2$, and $LaGa_{0.4}Sn_{0.4}Sb_2$; and (c) $LaSn_{0.75}Sb_2$.

ACKNOWLEDGMENTS

The Natural Sciences and Engineering Research Council of Canada and the University of Alberta supported this work. We thank Dr. Robert McDonald (Faculty Service Officer, X-ray Crystallography Laboratory) for the data collection and Christina Barker for assistance with the EDX analysis.

REFERENCES

1. G. Cordier, H. Schäfer, and P. Woll, *Z. Naturforsch. B: Anorg. Chem. Org. Chem.* **40,** 1097 (1985).
2. A. Leithe-Jasper and P. Rogl, *J. Alloys Compd.* **203,** 133 (1994).
3. O. Sologub, K. Hiebl, P. Rogl, H. Noël, and O. Bodak, *J. Alloys Compd.* **210,** 153 (1994).
4. O. Sologub, H. Noël, A. Leithe-Jasper, P. Rogl, and O. I. Bodak, *J. Solid State Chem.* **115,** 441 (1995).
5. O. Sologub, K. Hiebl, P. Rogl, and O. Bodak, *J. Alloys Compd.* **227,** 40 (1995).
6. M. Brylak, M. H. Möller, and W. Jeitschko, *J. Solid State Chem.* **115,** 305 (1995).
7. P. Wollesen, W. Jeitschko, M. Brylak, and L. Dietrich, *J. Alloys Compd.* **245,** L5 (1996).
8. M. J. Ferguson, R. W. Hushagen, and A. Mar, *Inorg. Chem.* **35,** 4505 (1996).
9. M. J. Ferguson, R. E. Ellenwood, and A. Mar, *Inorg. Chem.* **38,** 4503 (1999).
10. A. M. Mills and A. Mar, *J. Am. Chem. Soc.* **123,** 1151 (2001).
11. R. Wang and H. Steinfink, *Inorg. Chem.* **6,** 1685 (1967).
12. R. Wang, R. Bodnar, and H. Steinfink, *Inorg. Chem.* **5,** 1468 (1966).
13. F. Hulliger and R. Schmelczer, *J. Solid State Chem.* **26,** 389 (1978).

14. A. M. Mills and A. Mar, *Inorg. Chem.* **39,** 4599 (2000).
15. G. M. Sheldrick, "SHELXTL," Version 5.1, Bruker Analytical X-ray Systems, Inc. Madison, WI, 1997.
16. A. J. C. Wilson, Ed., "International Tables for X-ray Crystallography," Vol. C. Kluwer, Dordrecht, 1992.
17. L. M. Gelato and E. Parthé, *J. Appl. Crystallogr.* **20,** 139 (1987).
18. G. Cordier, H. Ochmann, and H. Schäfer, *Mater. Res. Bull.* **21,** 331 (1986).
19. W. Blase and G. Cordier, *Z. Naturforsch. B: Anorg. Chem. Org. Chem.* **43,** 1017 (1988).
20. C. Kolm, S. A. Kulin, and B. L. Averbach, *Phys. Rev.* **108,** 965 (1957).
21. B. Eisenmann and J. Klein, *Z. Naturforsch. B: Anorg. Chem. Org. Chem.* **43,** 1156 (1988).
22. G. A. Papoian and R. Hoffmann, *Angew. Chem. Int. Ed.* **39,** 2408 (2000).
23. G. Papoian and R. Hoffmann, *J. Am. Chem. Soc.* **123,** 6600 (2001).
24. A. M. Mills, R. Lam, M. J. Ferguson, L. Deakin, and A. Mar, *Coord. Chem. Rev.*, in press.